

10<sup>th</sup> International Conference on Solid State Chemistry, Pardubice, Czech Republic

## Atmospheric-pressure microwave torch discharge generated $\gamma$ -Fe<sub>2</sub>O<sub>3</sub> nanopowder

B. David<sup>a\*</sup>, O. Schneeweiss<sup>a</sup>, N. Pizúrová<sup>a</sup>, Šantavá<sup>b</sup>, V. Kudrle<sup>c</sup>, P. Synek<sup>c</sup>,  
O. Jašek<sup>c</sup>

<sup>a</sup>CEITEC IPM, Institute of Physics of Materials, AS CR, v.v.i., Žitkova 22, CZ-61662 Brno, Czech Republic

<sup>b</sup>Institute of Physics, AS CR, v.v.i., Na Slovance 2, CZ-18221 Prague, Czech Republic

<sup>c</sup>Department of Physical Electronics, Faculty of Science, Masaryk University, Kotlářská 2, CZ-61137 Brno, Czech Republic

---

### Abstract

Microwave torch discharge ignited in Ar at 1 bar was used for the synthesis of  $\gamma$ -Fe<sub>2</sub>O<sub>3</sub> nanoparticles. A double-walled nozzle electrode enabled to introduce gases separately: Ar flowed in the central channel, whereas the mixture of H<sub>2</sub>/O<sub>2</sub>/Fe(CO)<sub>5</sub> was added into the torch discharge through an outer channel. The composition and properties of the synthesized nanopowders were studied by TEM, XRD, Raman and Mössbauer spectroscopies. Basic magnetic measurements at low/high temperatures were performed. The  $\gamma$ -Fe<sub>2</sub>O<sub>3</sub> phase with the mean crystallite size of 24 nm was identified by XRD in the representative sample. The measured Raman spectrum matched well those reported for  $\gamma$ -Fe<sub>2</sub>O<sub>3</sub> powders in the literature. In the transmission Mössbauer spectrum measured at 5 K the two sextets characteristic for  $\gamma$ -Fe<sub>2</sub>O<sub>3</sub> were clearly identified. No change in specific magnetic moment typical of Fe<sub>3</sub>O<sub>4</sub> at its Verwey temperature was observed on the zero field curve, which smoothly increased with temperature. Neither Fe<sub>3</sub>O<sub>4</sub> nor  $\alpha$ -Fe<sub>2</sub>O<sub>3</sub> were present in the sample. We also report on the high-temperature magnetic properties of the representative sample and describe its structural changes and phase transformations up to 1073 K.

© 2013 The Authors. Published by Elsevier B.V. Open access under [CC BY-NC-ND license](https://creativecommons.org/licenses/by-nc-nd/4.0/).

Selection and/or peer-review under responsibility of the Organisation of the 10th International Conference on Solid State Chemistry.

*Keywords:* Microwave discharge, maghemite, Mössbauer spectroscopy, magnetic measurements;

---

### 1. Introduction

Over the past years, a lot of work has been done on the synthesis of  $\gamma$ -Fe<sub>2</sub>O<sub>3</sub> (maghemite) particles because of their potential applications for ferrofluid, magnetic refrigeration, bioprocessing, information storage and gas sensitive materials [1]. Maghemite has spinel structure with two magnetically nonequivalent interpenetrating sublattices and exhibits ferrimagnetic behavior [2]. Its structural formula is [Fe<sup>3+</sup>]<sub>A</sub>[Fe<sup>3+</sup><sub>5/3</sub>□<sub>1/3</sub>]<sub>B</sub>O<sub>4</sub> and it differs from Fe<sub>3</sub>O<sub>4</sub> (magnetite) by the presence of cationic vacancies □ within

octahedral B sites. Nanoparticles can be also synthesized in a wide range of plasma processes, which can be classified e.g. by gas temperature and pressure. At atmospheric pressure, maghemite particles have been synthesized using the vaporized  $\text{Fe}(\text{CO})_5$  carried by argon gas and pyrolyzed either in the oxygen plasma generated by microwave plasma jet [3] or in the argon plasma generated by microwave torch discharge [4]. In the present paper the magnetic properties of a  $\gamma\text{-Fe}_2\text{O}_3$  nanopowder synthesized by the plasma method used in the Reference 4 are studied.

## 2. Experimental

The apparatus consisted of a microwave generator working at 2.45 GHz powering a double-walled nozzle electrode (via a broadband transition to a coaxial line by means of a ridge waveguide) over which a discharge was ignited [4,5,6]. Argon flowed through the central nozzle (700 sccm) and the mixture of  $\text{H}_2$  (250 sccm) and  $\text{Fe}(\text{CO})_5$  vapour was added into the Ar discharge through the outer concentric nozzle. Vapour of liquid  $\text{Fe}(\text{CO})_5$  was entrained into the discharge by Ar (280 sccm) flowing over its surface. The power used during the experiment was 140 W. The nanopowder was collected on reactor walls and labelled T96. Transmission electron microscopy (TEM) was performed on a Philips microscope CM12 (W cathode, 120 kV electron beam). Phase composition was studied by X-ray diffraction (XRD) on a PANalytical X'Pert Pro MPD device (Co  $K\alpha$ ). XRD pattern fitting was done using a commercial software and a database and it yielded mean crystallite size  $d_{\text{XRD}}$  for a given phase [7].

Mössbauer spectra (MS) were obtained at standard transmission geometry with  $^{57}\text{Co}$  in Rh matrix source. As a result of the fitting procedure performed with CONFIT [8] we obtained the value of relative spectrum area  $A$  for a given phase and spectral component parameters: hyperfine magnetic induction  $B_{\text{HF}}$ , quadrupole shift  $\varepsilon_Q$ , quadrupole splitting  $\Delta E_Q$  and isomer shift  $\delta$  (against  $\alpha\text{-Fe}$ ).

A CCS-800 closed-cycle refrigerator system from Janis was used for low-temperature Mössbauer measurements. A PPMS 9T system from Quantum Design (with ACMS option) was employed for low-temperature magnetic measurements. High-temperature magnetic measurements were done on an EG&G PARC vibrating sample magnetometer.

## 3. Results

The XRD pattern for T96 sample (Fig. 1a) was fitted with cubic maghemite-C with ordered vacancies (ICSD #87119, unit cell  $a = 0.8345$  nm, space group  $P4_332$ ) with the result:  $a = 0.8358$  nm,  $d_{\text{XRD}} = 24$  nm. As the same fit could be obtained with tetragonal maghemite-Q with disordered vacancies (ICSD #87121, unit cell  $a = b = 0.8346$  nm,  $c = 25.034$  nm, space group  $P4_32_12$ ), the sample could be a mixture of both. Compared to  $\text{Fe}_3\text{O}_4$  (ICSD #75627, unit cell  $a = 0.8397$  nm, space group  $\text{Fd-}3\text{mZ}$ )  $\gamma\text{-Fe}_2\text{O}_3$  has distinctive lines at  $2\theta = 17.5^\circ, 27.8^\circ, 30.5^\circ, 58.9^\circ, 85.4^\circ$  which are not present in the XRD pattern of  $\text{Fe}_3\text{O}_4$ . Because the lines of  $\text{Fe}_3\text{O}_4$  are a subset of  $\gamma\text{-Fe}_2\text{O}_3$  lines, the presence of  $\text{Fe}_3\text{O}_4$  in the sample could not be excluded. A very low-intensity peak at  $2\theta = 52.5^\circ$  was assigned to the main diffraction line of  $\alpha\text{-Fe}$  (ICSD #53451).

Generally, the Raman bands of  $\gamma\text{-Fe}_2\text{O}_3$  are not well defined and the resolution is directly related to the degree of crystallinity of the material studied. Raman spectrum of the sample (Fig. 1b) well agrees with the spectrum of another sample produced by the same synthesis method [4]. Based on this measurement, however, the presence of  $\text{Fe}_3\text{O}_4$  (which has the main peak at  $670\text{ cm}^{-1}$  and smaller peaks at  $300$  and  $534\text{ cm}^{-1}$ ) could not be excluded in the studied sample.

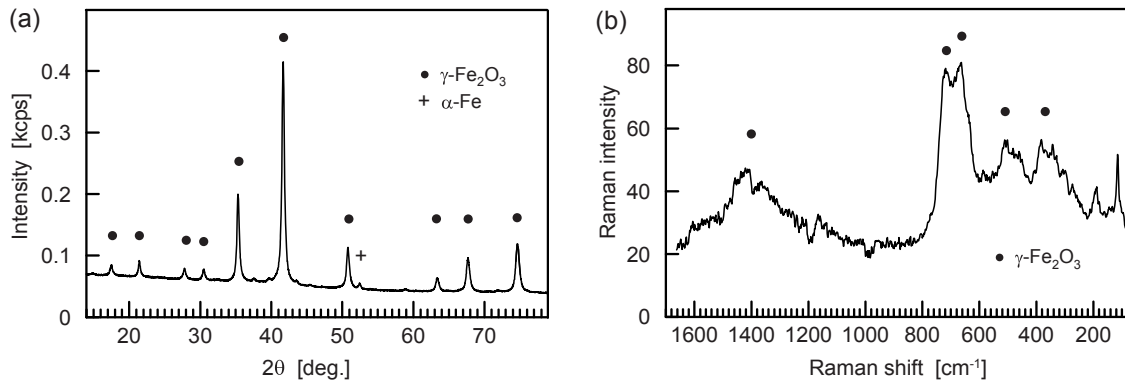


Fig. 1. (a) X-ray diffraction pattern and (b) Raman spectrum for T96 sample

Characteristic powder morphology and particle sizes can be observed in the Figure 2. Although particles smaller than  $\sim 30$  nm prevail, larger particles with diameters up to  $\approx 200$  nm could be found in the TEM images. It was also observed that some smaller particles formed chains. The diffraction rings in electron powder diffractograms were undoubtedly assigned to  $\gamma\text{-Fe}_2\text{O}_3/\text{Fe}_3\text{O}_4$ .

Mössbauer spectrum (MS) of maghemite (spinel structure with two sublattices) consists of two sextets [2]. As can be seen in the Figure 3a, the integral spectrum area ( $I_{SA}$ ) was six times higher at 5 K (measured for 2 days; cryostat was on) than at 293 K (10-days spectrum; cryostat was off). The anomalous decrease of the absorption at 293 K is attributed to the thermal motion of small particles and chain-like morphology of very small particles, which enables diffusive tilting motions of  $\gamma\text{-Fe}_2\text{O}_3$  nanoparticles [9]. Similar decrease was observed for a nanopowder synthesized in low-pressure microwave plasma [10] and in case of a nanopowder synthesized by laser pyrolysis method [10]. In the MS measured at 293 K, due to small absorption, a doublet ( $\Delta E_Q = 0.40$  mm/s,  $\delta = 0.21$  mm/s, dashed line) and a singlet ( $\delta = 0.41$  mm/s; full line) were visible. They belong to Fe impurities in the Al foil in which the nanopowder was wrapped [12]. Spectral components characteristic for superparamagnetic relaxation surprisingly did not appear in this spectrum [13].

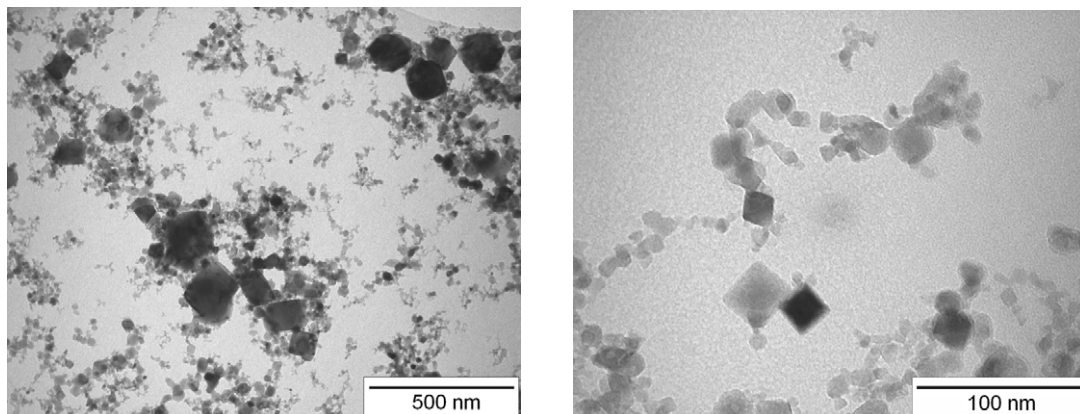


Fig. 2. Transmission electron images with different magnifications for T96 sample

The MS measured at 5 K, which was decisive for phase assessment, was fitted with Fe<sub>A</sub> sextet ( $B_{HF} = 51.0$  T,  $\varepsilon_Q = -0.02$  mm/s,  $\delta = 0.39$  mm/s,  $A = 0.30$ , dashed line), Fe<sub>B</sub> sextet ( $B_{HF} = 52.9$  T,  $\varepsilon_Q = 0.01$  mm/s,  $\delta = 0.49$  mm/s,  $A = 0.64$ , full line), S1 sextet ( $B_{HF} = 45.8$  T,  $\varepsilon_Q = -0.13$  mm/s,  $\delta = 0.61$  mm/s,  $A = 0.04$ , full line), an insignificant  $\alpha$ -Fe sextet ( $B_{HF} = 33.9$  T,  $\varepsilon_Q = 0.00$  mm/s,  $\delta = 0.14$  mm/s,  $A = 0.01$ , black filler), and low-intensity Fe<sup>2+</sup> singlet ( $\delta = 0.32$  mm/s,  $A = 0.01$ , thin line). It means that 32 % of Fe<sup>3+</sup> ions in  $\gamma$ -Fe<sub>2</sub>O<sub>3</sub> occupied tetragonal A sites. The S1 sextet belongs to not fully oxidized Fe<sub>3</sub>O<sub>4</sub>.

Vibrational motion of Fe atoms influences absorption, i.e. integral spectrum area ( $I_{SA}$ ), of a Mössbauer spectrum. This dependence is described by the Lamb-Mössbauer recoilless factor (LMRF), whose derivation is based on the Debye model of heat capacity of a solid, so the characteristic Debye temperature ( $\theta_D$ ) of a solid appears as a parameter in the LMRF [13,14]. Because of this the heat capacity measurement was performed (Fig. 3b). For each point on the  $C_p$  curve, the  $\theta_D$  was calculated according to the Debye model and it is shown in the Figure 3b. Because  $\theta_D$  grew strongly with increasing temperature from  $\theta_D(2\text{ K}) = 241$  K up to  $\theta_D(231\text{ K}) = 617$  K, it seems that the Debye model does not describe the  $C_p$  of the nanopowder in the range 2–300 K properly. Nevertheless, the value  $\theta_D(2\text{ K}) = 241$  K is close to the reference value for  $\gamma$ -Fe<sub>2</sub>O<sub>3</sub> which was reported to be 225 K [15]. The measured value  $C_p(293\text{ K}) = 104$  J/K/mol agrees very well with the reference value of 103.9 J/K/mol determined for  $\gamma$ -Fe<sub>2</sub>O<sub>3</sub> at 293 K [16]. In the inset in the Figure 3b, the  $C_p$  in the interval 4–40 K was fitted with the Einstein and Debye low-temperature terms:  $C_p = 2.51 \cdot 10^{-3} T^2 + 4.14 \cdot 10^5 T^3$  [J/K/mol].

A loose nanopowder was pressed into pellets for magnetic measurements. The parameters of the hysteresis loop (HL) measured at 293 K (Fig. 4a) were:  $H_C = 12.5$  kA/m,  $\sigma_R = 16.1$  Am<sup>2</sup>/kg,  $\sigma_S = 66.6$  Am<sup>2</sup>/kg (at 795 kA/m). The reference value of  $\sigma_S$  for  $\gamma$ -Fe<sub>2</sub>O<sub>3</sub> is 82 Am<sup>2</sup>/kg [13].

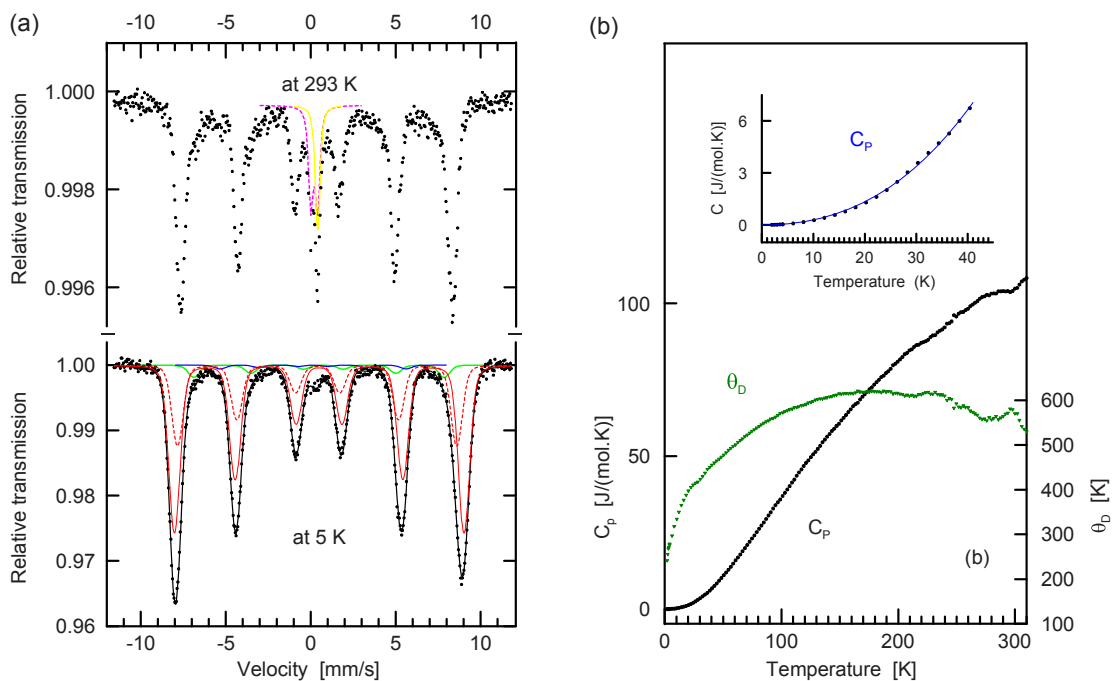


Fig. 3. (a) Mössbauer spectra measured at the indicated temperatures and (b) heat capacity  $C_p$ , calculated Debye temperature  $\theta_D$ , and the fit of  $C_p$  at low temperature (in the inset) for T96 sample

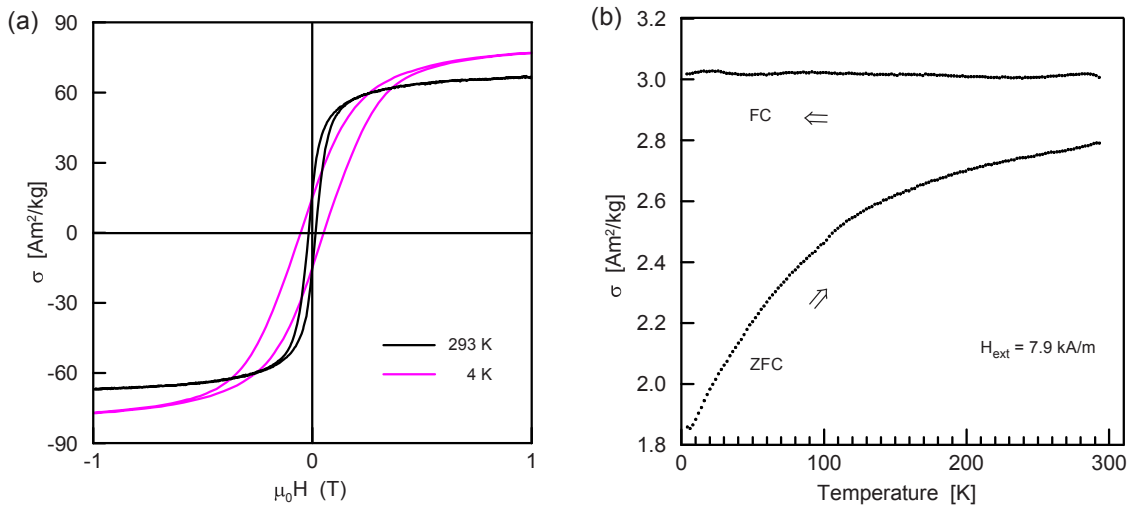


Fig. 4. (a) Hysteresis loops and (b) ZFC/FC curves for T96 sample

The measured zero field cooled (ZFC) and field cooled (FC) curves (Fig. 7) showed the split between  $\sigma_{ZFC}$  (which remains constant) and  $\sigma_{FC}$  curves over the whole measurement range.  $\sigma_{ZFC}$  exhibited no maximum but grew strongly with increasing temperature, i.e. particle magnetic moments tended to align in the direction of  $H_{\text{ext}}$ . We suppose that particles are strongly magnetically coupled, so superparamagnetic relaxation in small particles below 300 K was not possible. No features near 120 K (or below 120 K) which would have marked the Verwey transition in  $\text{Fe}_3\text{O}_4$  compound were present on the ZFC curve [17]. It confirms, together with previous results, that  $\text{Fe}_3\text{O}_4$  was not present in the sample. The HL measured at 4 K provided the values:  $H_C = 42.6$  kA/m,  $\sigma_R = 14.3$   $\text{Am}^2/\text{kg}$ ,  $\sigma_S = 77.0$   $\text{Am}^2/\text{kg}$  (at 795 kA/m).

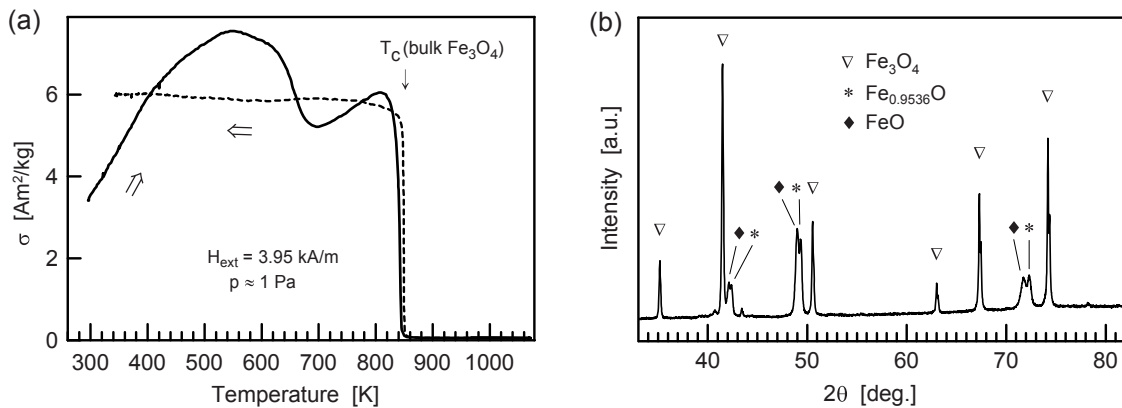


Fig. 5. (a) Thermomagnetic curve for T96 sample, (b) XRD pattern for T96 sample after its thermomagnetic curve measurement

By the thermomagnetic (TM) curve measurement (Fig. 5a) a pellet was held in an evacuated cell, heated up to 1073 K (hold time 30 min) and then cooled down. The Curie temperature  $T_C(\text{bulk-Fe}_3\text{O}_4) = 860$  K can be easily recognized on the TM curve [18]. When heating began at 300 K,  $\sigma$  grew up to 540 K. This increase was caused by the relaxation in  $H_{\text{ext}}$  and recrystallisation (XRD showed the same phases as at 293 K). The subsequent drop was probably due to the onset of  $\gamma\text{-Fe}_2\text{O}_3 \rightarrow \alpha\text{-Fe}_3\text{O}_4$  transformation and the following increase starting at 700 K was caused by  $\gamma\text{-Fe}_2\text{O}_3/\alpha\text{-Fe}_3\text{O}_4 \rightarrow \text{Fe}_3\text{O}_4$  reduction in vacuum and  $\text{Fe}_3\text{O}_4$  recrystallisation and growth (XRD showed only  $\text{Fe}_3\text{O}_4$  phase at 850 K). According to the equilibrium Fe-O phase diagram [19], wustite  $\text{Fe}_x\text{O}$  can form above 843 K.

After the whole TM measurement cycle, the XRD measurement showed (Fig. 5b) that the sample was a mixture of  $\text{Fe}_3\text{O}_4$  (PDF #1-88-866),  $\text{FeO}$  (PDF #1-89-7100) and  $\text{Fe}_{0.9536}\text{O}$  (PDF #1-74-1880), i.e. the reduction of the original  $\gamma\text{-Fe}_2\text{O}_3$  took place. The parameters of the HL measured at 293 K were:  $H_C = 2.7$  kA/m,  $\sigma_R = 3.5$  Am<sup>2</sup>/kg,  $\sigma_S = 69.0$  Am<sup>2</sup>/kg (at 795 kA/m), hence the annealed sample was magnetically softer than the synthesized powder ( $\text{Fe}_3\text{O}_4$  is ferrimagnetic and  $\text{FeO}$  is paramagnetic at room temperature).

#### 4. Conclusions

The results can be summarized as follows: the crystallite sizes of synthesized  $\gamma\text{-Fe}_2\text{O}_3$  nanoparticles varied from a few nanometers to 200 nm. The traces of  $\alpha\text{-Fe}$  (one XRD line, sextet with negligible intensity in the MS measured at 5 K) seem to be at unimportantly low level. According to the performed measurements (Mössbauer spectrum at 5 K, ZFC curve)  $\text{Fe}_3\text{O}_4$  is not present in the sample. On the other hand, the specific magnetization of the synthesized sample did not reach the tabulated value for pure maghemite, which could have different reasons. Nevertheless, it can be concluded that the atmospheric microwave torch discharge method is suitable for the synthesis of  $\gamma\text{-Fe}_2\text{O}_3$  nanoparticles.

#### Acknowledgements

This work was supported by the Grant Agency of the Czech Republic (104/09/H080, 205/10/1374, 106/08/1440, 202/08/0178), the Academy of Sciences of the Czech Republic (AV0Z20410507), and the Ministry of Education, Youth and Sport of the Czech Republic (MSM0021622411, 1M6198959201). This work was realized in CEITEC – Central European Institute of Technology with research infrastructure supported by the project CZ.1.05/1.1.00/02.0068 financed from European Regional Development Fund.

#### References

- [1] Kang YS, Risbud S, Rabolt JF, Stroeve P. Synthesis and characterization of nanometer-size  $\text{Fe}_3\text{O}_4$  and  $\gamma\text{-Fe}_2\text{O}_3$  particles. *Chem Mater* 1996;**8**:2209–2211 .
- [2] Tuček J, Zboril R, Petridis D. Maghemite nanoparticles by view of Mössbauer spectroscopy. *J Nanosci Nanotech* 2006;**6**: 926–947.
- [3] Li SZ, Hong YC, Uhm HS, Li ZK. Synthesis of nanocrystalline iron oxide particles by microwave plasma jet at atmospheric pressure. *Jpn J Appl Phys* 2004;**43**:7714–7717.
- [4] Synek P, Jašek O, Zajíčková L, David B, Kudrle V, Pizúrová N. Plasmachemical synthesis of maghemite nanoparticles in atmospheric pressure microwave torch. *Mat Lett* 2011;**65**:982–984.

- [5] Zajíčková L, Synek P, Jašek O, Eliáš M, David B, Buršík J, Pizúrová N, Hanzlíková R, Lazar L. Synthesis of carbon nanotubes and iron oxide nanoparticles in MW plasma torch with  $\text{Fe}(\text{CO})_5$  in gas feed. *Appl Surf Sci* 2009;**255**:5421–5424.
- [6] David B, Pizúrová N, Schneeweiss O, Kudrle V, Jašek O, Synek P. Iron-based nanopowders containing  $\alpha$ -Fe,  $\text{Fe}_3\text{C}$ , and  $\gamma$ -Fe particles synthesised in microwave torch plasma and investigated with Mössbauer spectroscopy. *Jpn J Appl Phys* 2011;**50**:08JF11.
- [7] X'Pert High Score Plus 2.0a, PANalytical BV, Lelyweg 1, Almelo, the Netherlands. ICSD Database release 2010/2, FIZ Karlsruhe, Germany; PDF-2 database, release 54 (2004), International Centre for Diffraction Data, Newton Square, PA, USA.
- [8] Žák T, Jirášková Y. CONFIT: Mössbauer spectra fitting program. *Surf Interface Anal* 2006;**38**:710–714.
- [9] von Eynatten G, Ritter T, Bömmel HE, Dransfeld K. Diffusive motion of iron microcrystals studied by Mössbauer spectroscopy. *Z Phys B Cond Matter* 1987;**65**:341–345.
- [10] David B, Pizurova N, Schneeweiss O, Šantavá E, Jašek O, Kudrle V.  $\alpha$ -Fe nanopowder synthesised in low-pressure microwave plasma and studied by Mössbauer spectroscopy. *J Phys: Conf Ser* 2011;**303**:012090.
- [11] David B, Pizúrová N, Schneeweiss O, Klementová M, Šantavá E, Dumitrache F, Alexandrescu R, Morjan I. Magnetic properties of nanometric Fe-based particles obtained by laser-driven pyrolysis. *J Phys Chem Solids* 2007;**68**:1152–1156.
- [12] Nasu S, Gonser U, Shingu PH, Murakami Y.  $^{57}\text{Fe}$  Mössbauer spectra in splat-quenched Al-0.5,1,3 and 5 at% Fe alloys. *J Phys F: Metal Phys* 1974;**4**:L24–L28.
- [13] Güttlich P, Bill E, Trautwein AX. *Mössbauer spectroscopy and transition metal chemistry*. Berlin: Springer-Verlag; 2011.
- [14] Patterson J, Bailey BC. *Solid state physics: introduction to the theory*. Berlin: Springer-Verlag; 2007.
- [15] Mørup S, Dumensic JA, Topsøe H. Magnetic microcrystals. In: Cohen RL, editor. *Applications of Mössbauer spectroscopy, Vol. II*, New York: Academic Press; 1980. p. 1–53
- [16] Majzlan J, Lang BE, Stevens R, Navrotsky A, Woodfield BF, Boerio-Goates J. Thermodynamics of iron oxides: Part I. Standard entropy and heat capacity of goethite ( $\alpha$ - $\text{FeOOH}$ ), lepidocrocite ( $\gamma$ - $\text{FeOOH}$ ), and maghemite ( $\gamma$ - $\text{Fe}_2\text{O}_3$ ). *Am Mineral* 2003;**88**:846–854.
- [17] Goya GF, Berquo TS, Fonseca FC, Morales MP. Static and dynamic magnetic properties of spherical magnetite nanoparticles. *J Appl Phys* 2003;**94**:053520-9.
- [18] Coey JMD. *Magnetism and magnetic materials*. Cambridge, Cambridge university press; 2009.
- [19] Binary Alloy Phase Diagrams, 2nd ed. plus updates. ASM International, Materials Park, Ohio, U.S.A., 1996.